Available online at www.sciencedirect.com

SCIENCE DIRECT®

Solid State Ionics 175 (2004) 39–46

SOLID STATE IONICS

www.elsevier.com/locate/ssi

Anode-supported thin-film fuel cells operated in a single chamber configuration 2T-I-12

Zongping Shao, Chan Kwak, Sossina M. Haile*

Materials Science, California Institute of Technology, Pasadena, CA 91125, United States

Received in revised form 10 May 2004

Abstract

The performance characteristics of anode-supported, thin-film, single chamber fuel cells (SCFCs) have been investigated. Cells, in which Ni+$Sm_{0.15}Ce_{0.85}O_2$ (Samaria doped ceria, SDC) served as the anode and SDC as the electrolyte, were fabricated by dry pressing. High quality, bilayer structures with electrolyte thicknesses as small as 10 μm were prepared with excellent reproducibility. The cathode, 70 wt.% $Sm_{0.5}Sr_{0.5}CoO_3$+30% SDC, was deposited by a spray method. The cells were operated in a dilute propane+oxygen mixture. The influence of environmental temperature, gas composition and flow rate on the fuel cell performance were investigated. At low temperatures, fuel cell power output was limited primarily by poor catalytic activity at the anode whereas at high temperatures it was limited primarily by high catalytic activity of the cathode towards propane oxidation. Thus, intermediate temperatures are optimal for maximizing power densities. An increase in fuel flow rate led to an increase of the fuel cell temperature due to exothermal partial oxidation on the anode, producing a complex response in fuel cell power output. Under optimized gas compositions and flow conditions, a peak power density of ~210 mW/cm^2 was obtained.

Keywords: Single chamber fuel cell (SCFC); Samaria doped ceria (SDC); $Sm_{0.5}Sr_{0.5}CoO_3$ (SSC); Anode-supported fuel cell

1. Introduction

While solid oxide fuel cells (SOFCs) exhibit a number of attractive features for power generation, including high energy conversion efficiency, fuel flexibility and relatively inexpensive electrode materials, the high temperatures required for operation (800–1000 °C) introduce a number of challenges. In particular, for planar SOFCs, thermal expansion mismatches between components can lead to failure of the seals that separate anode and cathode chambers. One strategy for addressing this challenge is to lower the temperature of operation, a strategy that bears additional benefits in terms of lowering fuel cell costs by enabling the use of lower cost metals to replace selected ceramic components. A second strategy is to utilize so-called 'single chamber fuel cells' (SCFCs) in which the fuel and oxidant are allowed to mix and anode and cathode reactions take place within the same physical chamber [1].

Single chamber fuel cells rely on the different chemical catalytic and electrocatalytic activities of anode and cathode materials for their operation. High open circuit voltages (OCVs) of ~0.9 V and power densities of ~400 mW/cm^2 at 500 °C were reported by Hibino et al. [1] for thick-film fuel cells based on samaria doped ceria and operated in single chamber mode using an ethane–air mixture. Their results suggest that the primary losses of the cell at lower temperatures originated from the thick electrolyte. In the present work, we report results on the performance of anode-supported, thin electrolyte fuel cells operated in a single chamber configuration, in which propane and oxygen, diluted with helium, served as the gas mixture.

* Corresponding author. Fax: +1 626 395 3933.
E-mail address: smhaile@caltech.edu (S.M. Haile).

0167-2738/$ - see front matter © 2004 Elsevier B.V. All rights reserved.
doi:10.1016/j.ssi.2004.09.018

2. Fuel cell fabrication

In analogy to earlier studies [1], the electrolyte and anode components of the fuel cell of the present investigation were comprised, respectively, of 15% samaria doped ceria (SDC) and of Ni+SDC (NiO:SDC=50–60:40–50 wt.%) cermets. As the cathode, a composite of 30 wt.% SDC+70 wt.% $Sm_{0.5}Sr_{0.5}CoO_{3-\delta}$ (SSC) was utilized. In general terms, the anode–electrolyte–cathode trilayer structure was fabricated by first pressing the anode-supported anode–electrolyte bilayer followed by sintering and anode reduction. The cathode was then spray deposited and sintered under inert atmosphere. The disc shaped fuel cells had a final diameter of 13.3 mm, an anode porosity of ~50% and thickness of ~0.7 mm, an electrolyte thickness between 10 and 20 μm, and a cathode thickness of 5–10 μm and surface area of 0.71 cm^2. An SEM image of a typical electrolyte–anode bilayer prepared by dual pressing is presented in Fig. 1.

Details of the fuel cell fabrication process are as follows. For the anode, high surface area SDC from NexTech (~180 m^2/g), synthesized by a hydrothermal method, or in-house prepared SDC, synthesized by an EDTA-citrate method [2] (calcined at 550 °C for 23 h, surface area of ~18 m^2/g), was combined with NiO from Alfa Aesar (green, particle size <35 μm) and/or NiO from Aldrich (black, particle size <10 μm). In order to control the porosity of the anode, an organic additive was sometimes added to the anode powder; specifically, water soluble PVP 8000 was utilized for this purpose, with the content ranging from 0% to 14%. The in-house synthesized SDC (EDTA-citrate derived, pre-calcined at 600 °C, 23 h) was used as the electrolyte layer material. For bilayer preparation, about 0.5 g of anode powder (<200 mesh) was first pressed using a 15 mm stainless steel die under a 1.5 ton load (83 MPa), then an appropriate quantity of SDC powder added to serve as the electrolyte layer and the bilayer pressed again under an 8 ton load (440 MPa). The green, dual-layer cells were calcined at 1200–1400 °C for 3–5 h under ambient air atmosphere, and subsequently annealed in flowing, diluted hydrogen at 600 °C for 6 h in order to reduce the NiO in the anode to Ni prior to the cathode deposition. In situ reduction of the anode, as is typical in conventional dual chamber fuel cells, is not possible in the single chamber configuration because the cathode would also be reduced. The cathode particles were suspended in a mixture of isopropyl alcohol, ethylene glycol and glycerin, deposited onto the electrolyte surface by spraying, and then calcined at 1000 °C (N_2 or Ar) for 5 h, conditions which was found to give good adhesion between the cathode and the electrolyte. In all, careful optimization of the SDC surface area and green packing density and of the shrinkage properties of both the anode and electrolyte was necessary in order to succeed in obtaining pinhole free SDC electrolyte films, 10–20 μm in thickness. To the complete trilayer structures, silver gauze was applied using silver conductive paste (Alfa Aesar) to serve as current collectors. In order to increase the electronic conductivity of the cathode, its entire surface was covered with a thin layer of colloidal silver ink (Ted Pella).

3. Chemical and electrochemical characterization

The chemical catalytic activity of anode and cathode materials for propane oxidation was tested in both flow-through and half-cell configurations using the reactor shown schematically in Fig. 2. For flow-through experiments, ~0.05 g of anode powder (calcined at 600 or 1350 °C) ~0.2 g of cathode powder (calcined at 600–1000 °C) was mixed with 1.5 g inert quartz sand (100–120 mesh) to minimize the temperature inhomogeneity within the catalyst bed. The effluent gas from the reactor was then directed to a Varian CP 4900 microgas chromatograph for in situ composition analysis. For fuel cell experiments, polarization curves were measured using a Keithley 2420 source meter interfaced with a computer and controlled under Labview 6.1 software. Power densities were calculated based on the cathode surface area (which was typically 0.71 cm^2 as compared to 1.39 cm^2 for the electrolyte). In addition, thermochemical calculations were carried out for comparison with the

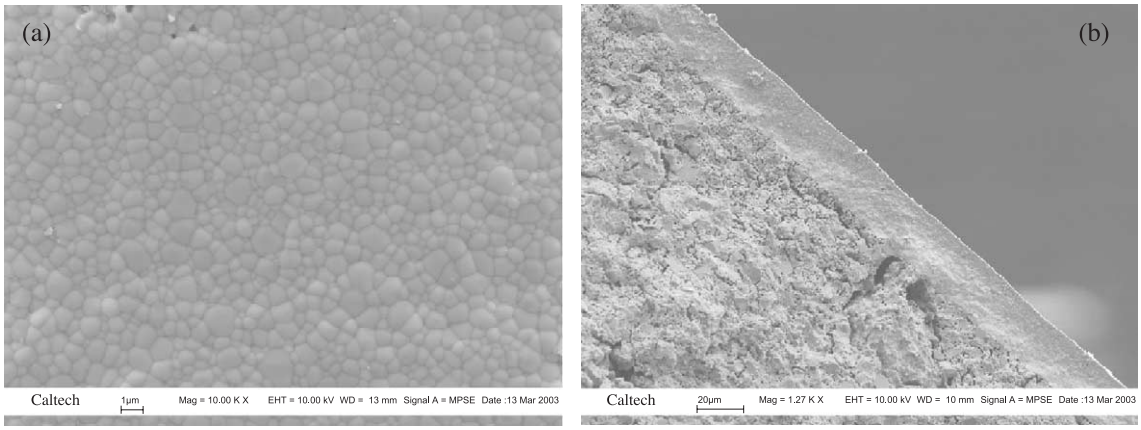

Fig. 1. SEM image of an anode–electrolyte bilayer half-cell fabricated as described in the text, (a) the SDC electrolyte surface, (b) the NiO-SDC|SDC bilayer (anode before reduction). The electrolyte has a thickness of ~20 μm.

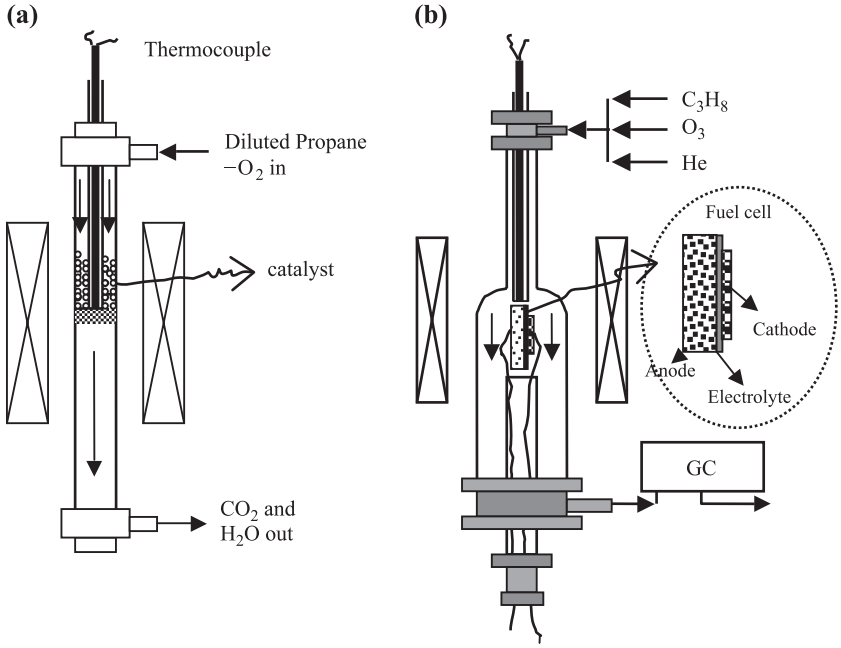

Fig. 2. Configuration of (a) the flow-through reactor for cathode and anode catalytic activity measurements, and (b) the reactor for half-cell catalytic activity and single chamber fuel cell measurements.

experimental data using the commercial chemistry software package HSC (Version 5.1, Outokumpu Research Oy, Finland).

4. Optimization of operating conditions: temperature and gas composition

In an ideal single chamber fuel cell, the electrodes are entirely selective for the desired reactions. Specifically, the cathode catalyzes oxygen electroreduction but not oxidation of the fuel. Similarly, the anode catalyzes partial (but not complete) oxidation of the fuel to yield CO and H_2, and subsequently catalyzes the electro-oxidation of these products. Examination of the cathode material, $Sm_{0.5}Sr_{0.5}CoO_{3-\delta}$ (SSC) (0.2 g in powder form), showed it to exhibit moderate activity for propane oxidation, Fig. 3. An oxygen conversion of 10–60%, which varied with SSC surface area and oxygen to propane ratio, was typically observed at 400 to 600 °C. A typical result, obtained from powders calcined at 900 °C, is presented in Fig. 3. An increase in calcination temperature lead to a reduction in surface area and thereby lower oxygen conversion rates. In all cases, the oxygen was almost entirely consumed at temperatures higher than 650 °C (not shown in the figure), which is a result of result of increase in both the catalytic activity of SSC for propane oxidation and the extent of gas phase combustion. Thus, the cathode material restricts operation of single chamber fuel cells utilizing propane as a fuel to temperatures of lower than 650 °C. Conversion of oxygen over the anode material, reduced Ni+SDC (0.05g in powder form calcined at 600 °C), occurred at much lower

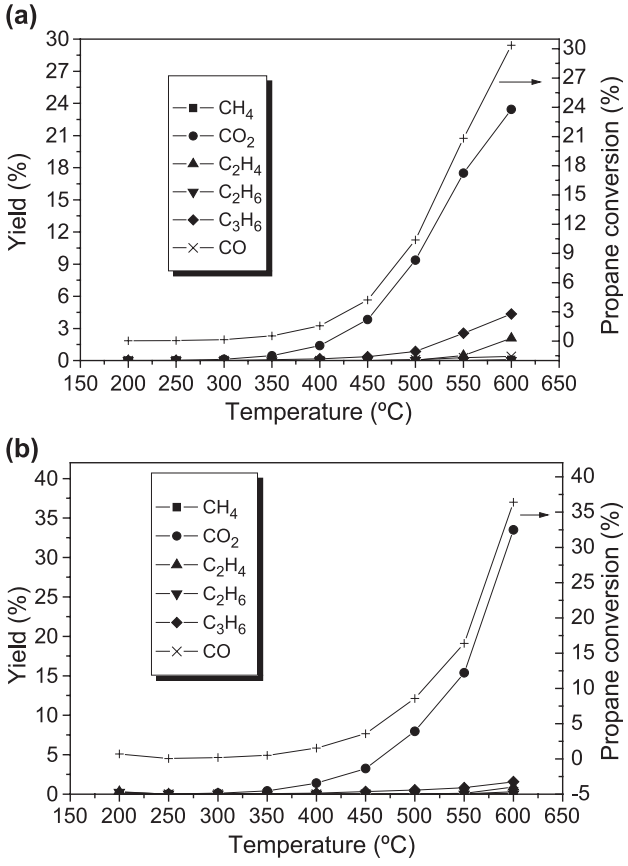

Fig. 3. Catalytic activity of SSC for propane oxidation, SSC pre-calcined at 900 °C for 5 h, 0.2 g, C_3H_8 flow rate of 1 ml/min [STP], helium flow rate of 200 ml/min [STP], (a) C_3H_8/O_2=1:1.5, and (b) C_3H_8/O_2=1:3.

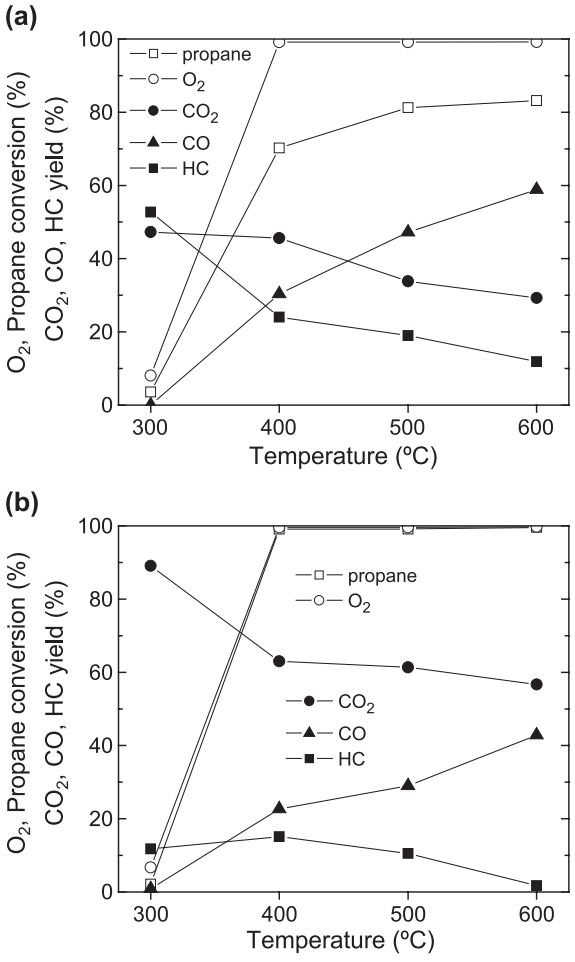

Fig. 4. Catalytic activity of Ni+SDC (0.05 g, calcined at 600°C) towards propane partial oxidation, C_3H_8 flow rate of 2 ml/min [STP], (a) C_3H_8/O_2/inert=1:1.6:6, and (b) C_3H_8/O_2/inert=1:3.2:12. Open symbols refer to conversion rates of the reactants and closed symbols to yields of the products. HC refers to all hydrocarbon species. The sample temperature is identical to that of the furnace.

temperatures, as desired, Fig. 4. Specifically, oxygen was completely converted to CO, CO_2 and H_2O by 400 °C. At temperatures lower than 400 °C, unreacted oxygen remained in the exhaust gas. Thus, the anode material restricts the operation of single chamber fuel cells utilizing propane as a fuel to temperatures of ~400 °C and above. Somewhat higher temperatures are advantageous for increasing the CO:CO_2 ratio, which might be expected to increase fuel cell power output. Not surprisingly, fuel rich mixtures also have the effect of increasing the CO:CO_2 ratio.

Because both anode and cathode reside within the same chamber in an SCFC, fuel cell operation is highly sensitive to gas transport between electrodes. Transport of the products of the anode partial oxidation reaction, CO and H_2, is particularly detrimental because these species can be expected to be readily oxidized on the perovskite cathode, even for cathodes which may be inactive towards propane oxidation. Similarly, replenishment of oxygen at the anode by transport from the cathode region is undesirable. The impact of gas transport was indirectly probed by placing electrolyte–anode half-cells in the catalytic reactor. The anode thickness of 700 μm is much smaller than the diameter of the reaction tube, 14 mm, and thus measurable oxygen conversion reflects significant gas transport in the radial direction. Conversion rates were measured over a range of C_3H_8:O_2 ratios, with a fixed propane flow rate of 10 ml/min [STP=standard temperature and pressure]. The results, shown in the form of the temperatures corresponding to 50% and 95% oxygen conversion rates as a function of gas mixture composition, are presented in Fig. 5. As discussed in detail below, the cell temperature is significantly higher (80–120 °C) that the furnace temperature, which is that reported in the figure. Substantial oxygen conversion indeed occurs at relatively low temperatures. Overall, however, the conversion rates are lower than in the flow-through reactor configuration. For C_3H_8:O_2=1:3, for example, 50% conversion of oxygen occurred at 475 °C (T_{anode} ~585 °C) in the half-cell configuration whereas complete conversion occurred at 400 °C in the flow-through configuration. This is in part due to the higher surface area of the material examined in the flow-through reactor due to the lower calcination temperature, and in part due to the different flow configuration, which limits the portion of the gas that passes through the anode in the half-cell experiment. Nevertheless, for C_3H_8:O_2=1:1 the oxygen was completely converted at T>475 °C in the half-cell configuration, demonstrating that at these temperatures essentially all of the gas passing through the reactor samples the pore space within the anode, despite the much larger cross-sectional area of the reactor tube furnace than that of the anode, and suggests that all product gases similarly escape from the anode and sample all regions of the reactor.

The combined effects of cathode catalytic activity, Fig. 3, anode catalytic activity, Fig. 4, suggest a limited tempe-

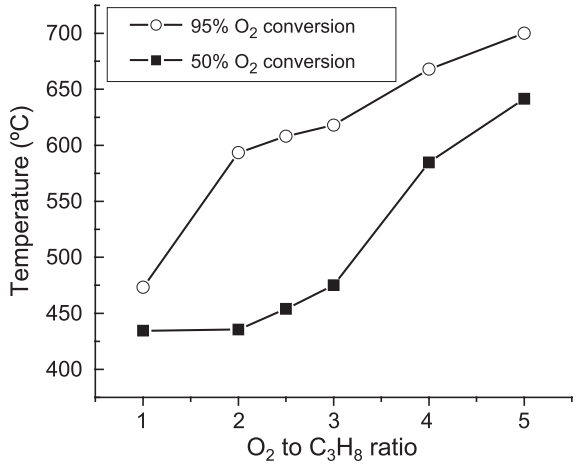

Fig. 5. The temperature at which selected levels of oxygen conversion were attained over an anode-supported half-cell (calcined at 1350 °C) as a function of the oxygen to propane ratio; propane feed rate fixed at 10 ml/min [STP], oxygen to helium ratio fixed at 1:4. The sample temperature is 80–120 °C higher than that of the furnace.

rature range for single chamber fuel cell operation. The temperature must be sufficiently high as to ensure that all of the oxygen that reaches the anode is totally consumed in the partial oxidation reaction, but low enough that cathode activity towards complete oxidation of the fuel is minimal. At high temperatures gas transport between electrodes, gas phase reactions, and electronic conductivity of the ceria electrolyte can also become problematic. The suitable temperature range for fuel cell operation depends not only on these parameters but also on the fuel to oxygen ratio and the overall flow rate. From a measurement of fuel cell power output (data not shown) using cells as described in Section 2 and a fixed propane flow rate of 10 ml/min [STP], it was generally observed that the operational temperature range (as set at the furnace) increased slightly from ~400 to 590 °C for C_3H_8:O_2=1:2 to ~400–650 °C for C_3H_8:O_2=1:5. An increase in the propane flow rate shifted the range further towards slightly higher temperatures. For example, at a propane flow rate of 40 ml/min [STP] the highest operational temperature was determined to be ~625 °C for a propane to oxygen ratio of 1:3, as compared to ~615 °C for a propane flow rate of 10 ml/min [STP].

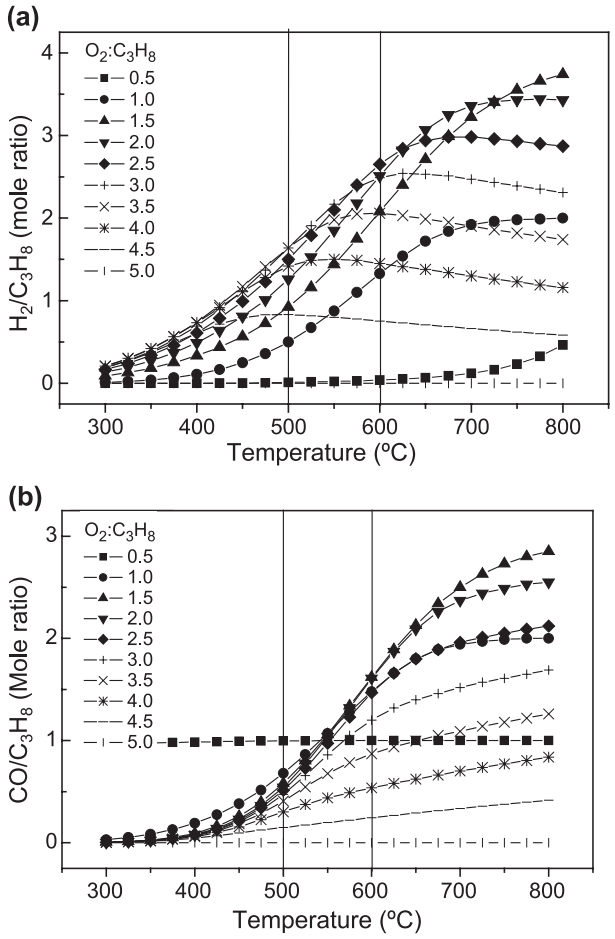

Fig. 6. Equilibrium (a) H_2 and (b) CO concentrations for a range of oxygen to propane ratios as functions of temperature, assuming no carbon deposition.

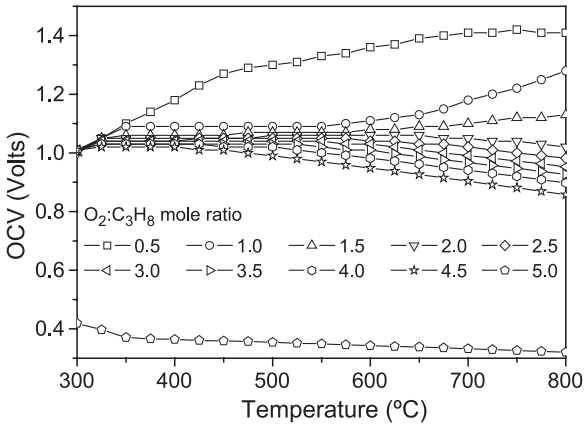

Fig. 7. Calculated OCV as function of temperature for various O_2/C_3H_8 ratios as indicated, under the assumptions of equilibrium gas concentration at the anode ignoring carbon deposition and input gas composition at the cathode. Little to no carbon deposition was observed in the fuel cell experiments.

The question of optimal operating conditions, in particular that of optimal oxygen to fuel ratio, can also be approached from a thermodynamic perspective. If one assumes that the gases in the vicinity of the anode reach thermodynamic equilibrium, the gas mixture at the anode can be calculated using the minimized total Gibbs free energy procedure. Of the gases present, H_2 and CO are the species of greatest relevance as these can presumably be directly electro-oxidized at the anode for power generation. The equilibrium concentrations of H_2 and CO as a function of temperature and oxygen to propane ratio, assuming no carbon deposition, are shown in Fig. 6. The assumption of no carbon deposition is justified by the fact that little to no coking was observed in these experiments. If one further assumes that the oxygen partial pressure at the cathode is that of the input gas mixture, it is then possible to calculate the expected open circuit voltage, Fig. 7. Under these idealized conditions, only stoichiometric mixtures yield low OCVs. All other mixtures result in voltages of 0.9 V or higher for the temperature range 300–800 °C. However, from the catalytic reactivity measurements, Figs. 3 and 4, however, it is clear that single chamber fuel cells comprised of the anode and cathode materials utilized here are viable over a measurably narrower temperature regime, ~400–700 °C (cell temperature). Within this range, the maximum H_2/C_3H_8 and CO:C_3H_8 ratios result from gas mixtures containing oxygen to propane ratios of about 2.5 to 3.0. Thus, under ideal conditions these mixtures would be anticipated to yield the highest SCFC power densities.

5. Fuel cell performance

All fuel cell experiments were carried out using the anode-supported Ni+SDC|SDC|SSC+SDC cells described above. Although several cells have been examined, the data presented are derived from three particular fuel cells.

Throughout this discussion, temperatures reported are those set at the furnace and not necessarily the temperature at the fuel cell. The open circuit voltage of cell-01 was examined under fixed gas flow conditions of 10 ml/min C_3H_8+30 ml/min O_2+120 ml/min He (all in STP), and over a range of temperatures, Fig. 8. As described below, under these conditions the cell anode temperature (as measured by placing a thermocouple in direct contact with the Ni+SDC anode) was 80–120 °C higher than the furnace temperature. At low temperatures, 425–450 °C (T_{anode} ~525–550 °C), open circuit voltages (OCVs) of only about 0.2 V were attained. Upon raising the temperature to 475 °C (T_{anode} ~575 °C), the OCV increased sharply to 0.65 V, and reached a maximum value of 0.85 V at 500 °C (T_{anode} ~610 °C), which corresponds to the highest OCV we have obtained to date from a single chamber fuel cell with C_3H_8+O_2+He as the feed gas. Beyond this temperature, the OCV decreased slowly over the range 500–625 °C (T_{anode} ~610–710 °C), and then dropped sharply to ~0.35 V at 650 °C (T_{anode} ~720 C) and almost zero at 675 °C (T_{anode} unknown).

For an anode that yields gas mixtures in thermodynamic equilibrium and the input gas mixture at the cathode, a theoretical OCV of 1.0–1.1 V is expected over this entire temperature regime, Fig. 7. The experimental value is much lower and follows the general temperature dependence expected from the catalytic activity measurements of Section 4. In particular, at low temperatures, Fig. 4, the catalytic activity of the anode towards propane partial oxidation is low, whereas at high temperatures, Fig. 3, the catalytic activity of the cathode for propane oxidation is high. Intermediate temperatures provide the optimal balance between these parameters. The mixed electronic and ionic conductivity of ceria, especially for the very thin electrolytes employed here, also causes a slight decrease in OCV from the theoretical value, but would not explain the temperature dependence observed. The high temperature limit for attaining high OCV in the fuel cells (T_{anode} ~710 °C, $T_{furnace}$ ~625°C) corresponds well to the limits implied by cathode catalytic activity (650 °C), Fig. 3, and the

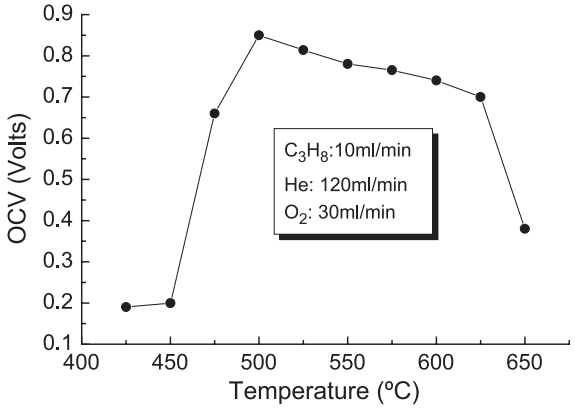

Fig. 8. Measured OCV as function of furnace set temperature (cell-01). Fuel cell anode temperature is ?.

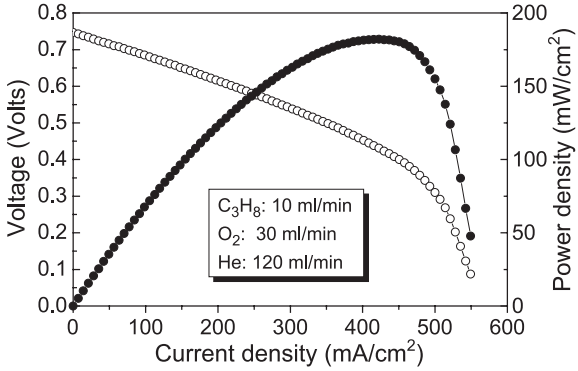

Fig. 9. Typical *I–V* and *I–P* characteristics for an Ni+SDC|SDC|SSC+SDC fuel cell operated at 525 °C (T_{anode} ~650 °C) in single chamber configuration; propane, oxygen and helium flow rates of 10, 30 and 120 ml/min [STP], respectively (cell-02).

effects of gas phase transport (T_{anode} ~710 °C, $T_{furnace}$ ~625°C), Fig. 5. The difference between the low temperature limit as determined from the OCV measurements (T_{anode} ~610 °C, $T_{furnace}$ ~475°C) and that implied by the catalytic activity of the anode material (400 °C), Fig. 4, is likely due to the higher surface area of the material employed in the catalytic activity measurements.

Representative *I–V* and *I–P* characteristics at 525 °C (T_{anode} ~650 °C) are shown in Fig. 9 for cell-02 exposed to gas flow conditions of 10 ml/min propane +30 ml/min oxygen+120 ml/min helium [all in STP]. These conditions were found to yield the highest peak power density for a fixed propane flow rate of 10 ml/min and a furnace temperature of 525 °C. The oxygen and helium flow rates that led to maximal values of peak power density varied with temperature (data not shown). The corresponding O_2:C_3H_8 ratios ranged from 1:3 to 1:3.5, in general agreement with the thermodynamic analysis of Section 4. Under optimized conditions, peak power density increased slightly from 500 to 525 °C (T_{anode} ~610–650 °C), reaching the maximum value of about ~185 mW/cm^2 shown in Fig. 9, and then remained constant at about 158 mW/cm^2 from 550 to 625 °C (T_{anode} ~660–710 °C). The temperature dependence of the OCV followed a trend similar to that of cell-01, despite the differing experimental conditions. Namely, the OCV first rose then fell with temperature, reaching its highest value at 525 °C (T_{anode} ~650 °C).

Cell-03 was utilized to probe the effect of propane feed rate on fuel cell power output. Measurements performed at a furnace temperature of 525 °C under fixed C_3H_8:O_2:He ratios of 1:3:12 (leaner mixture) and 1:2.5:10 (richer mixture), Fig. 10, demonstrated that, in general, peak power densities increased with increasing gas flow rates, although a slight decrease was observed at the highest flow rates for the leaner mixture. In contrast, the flow rate dependence of the OCV was very different for the two gas mixtures. While its value remained almost constant for the leaner mixture at ~0.7 V with a slight drop off at the highest flow rates, it sharply rose for the richer mixture

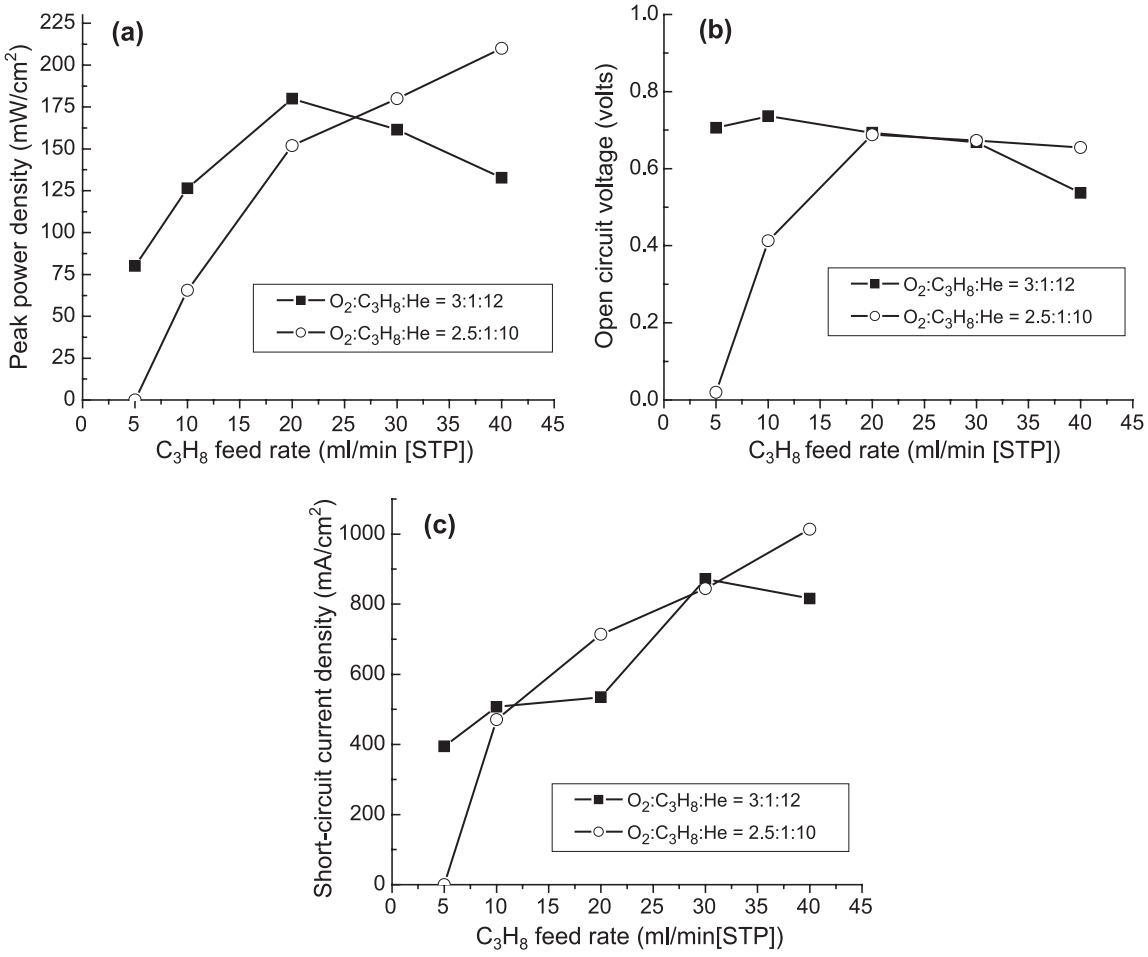

Fig. 10. The influence of propane feed rate and oxygen to propane ratio on single chamber fuel cell performance (cell-03); (a) peak power density, (b) open circuit voltage, and (c) current density at short circuit.

from essentially zero to ~0.65 V over the propane feed rate range of 5 to 15 ml/min, and then remained at this value at higher feed rates. The current density at short circuit exhibited an almost monotonic increase with gas feed rate for both mixtures. The highest power density achieved in this study, ~210 mW/cm^2, was attained using the fuel rich mixture of O_2:C_3H_8:He=2.5:1:10 and a propane feed rate of 40 ml/min [STP], Fig. 10a. Experimental limitations prevented investigation of higher flow rates, and such conditions may yield even power densities, but possibly at the cost of reduced fuel utilization. The results of Fig. 10 further demonstrate that while OCV measurements provide a reasonable screening of optimal conditions for fuel cell operation, maximum OCV and maximum peak power density do not occur under identical conditions.

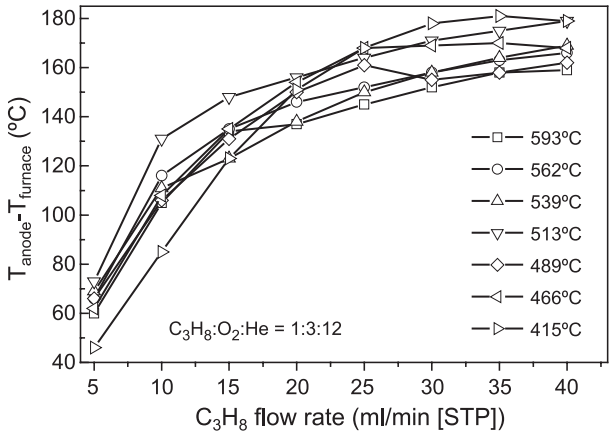

Fig. 11. The influence of propane flow rate on the rise in fuel cell temperature for the selected furnace temperatures indicated (cell-03). Overall gas composition held fixed as indicated.

The effects of gas feed rate are exerted, in large part, through changes in temperature at the fuel cell. Fig. 11 shows the fuel cell temperature relative to that of the furnace as measured at the anode, for various propane flow rates but at a constant gas ratio of C_3H_8:O_2:He=1:3:12. The fuel cell anode temperature was found to be 40–180 °C higher than the furnace set temperature, presumably as a result of the heat released during the exothermic partial oxidation reaction [3,4]. An increase in temperature would not only impact the catalytic activities of the anode and cathode as discussed earlier, Figs. 3 and 4, but would also increase the conductivity and electronic transference

number of the electrolyte. In addition, an increase in gas flow rate would tend of limit gas transport in the radial direction and counteract the increase in transport between electrodes otherwise observed for increasing temperatures, Fig. 5. Because of the multiple ways in which gas flow rate can impact fuel cell performance, it is difficult to assess which aspects are most responsible for the observed trends of Fig. 10.

6. Summary

Anode-supported SDC fuel cells with various cathodes were operated in a single chamber configuration under dilute propane–oxygen mixtures. The Ni+SDC anode is sufficiently active for propane partial oxidation at cell temperatures higher than 400–600 °C, whereas the SSC+SDC cathode is sufficiently inactive towards propane total oxidation only at cell temperatures below 650–700 °C. These facts, combined with increased gas transport between electrodes, increased electronic conductivity in the electrolyte and possible gas phase reactions at high temperatures, limit the operability range of SCFCs (comprised of the materials described here and operated as described here) to cell temperatures between approximately 600 and 700 °C. The operational parameters of propane to oxygen ratio and gas flow rate have pronounced effects on the fuel cell performance. The optimal propane to oxygen ratio is between 3 and 3.5, for low propane flow rates (10 ml/min), and corresponds well to expectations based on thermodynamic evaluations. An increase in overall (and thus propane) gas flow rates caused a dramatic increase in fuel cell temperature, producing a complex response of fuel cell performance to this parameter. In all, suppressing gas transport between anode and cathode and enhancing catalyst selectivity are essential for improving the fuel cell power output.

Acknowledgements

Dr. Ma Chi kindly assisted with electron microscopy. This work was funded by DARPA, Microsystems Technology Office. Additional support was provided by the National Science Foundation, Division of Materials Research, through its support of the Caltech Center for the Science and Engineering of Materials.

References

[1] T. Hibino, A. Hashimoto, T. Inoue, J. Tokuno, S. Yoshida, M. Sano, Science 288 (2000) 2031.
[2] Z.P. Shao, W.S. Yang, Y. Cong, H. Dong, J.H. Tong, G.X. Xiong, J. Membr. Sci. 172 (2000) 177.
[3] T. Hibino, A. Hashimoto, T. Inoue, J. Tokuno, S. Yoshida, M. Sano, J. Electrochem. Soc. 148 (2001) A544.
[4] T.W. Napporn, F. Morin, M. Meunier, Electrochem. Solid-State Lett. 7 (2004) A60.